Computing Elastic Constants for Random Polycrystals of Orthotropic $MgSiO_3$, Related Polymorphs, and $CaIrO_3$ Analogs

James G. Berryman[1,*]

[1] *University of California, Lawrence Berkeley National Laboratory, One Cyclotron Road MS 74R316C, Berkeley, CA 94720, USA*

(Dated: June 22, 2013)

Abstract

Recent advances in methods for computing both Hashin-Shtrikman bounds and related self-consistent (*i.e.*, coherent potential approximation, or CPA) estimates of the geomechanical constants for polycrystals composed of randomly oriented crystals have been successfully applied to orthotropic $MgSiO_3$-perovskite, post-perovskite, and some related $CaIrO_3$ analogs. In particular, Hashin-Shtrikman bounds provide significantly tighter constraints on the average polycrystal behavior than do the traditional Voigt and Reuss bounds. Self-consistent estimates of effective bulk and shear moduli always lie inside the Hashin-Shtrikman (HS) bounds, unlike the Voigt-Reuss-Hill estimates which might lie inside the HS bounds for some examples, but more typically lie outside these same Hashin-Shtrikman bounds. The discrepancies observed between Voigt-Reuss-Hill estimators and the self-consistent, geometric mean, or Hashin-Shtrikman estimates are nevertheless often small in the examples treated here, being on the order of about 1 percent or less — for both the effective bulk and shear moduli. Percentage discrepancies are also observed to be typically less for the effective shear modulus than for the bulk modulus. This result presumably follows from the method's implicit averaging over five distinct shear-like modes, including three true shear modes (due to twisting excitations) and two quasi-shear modes related to shearing action of uniaxially applied stress or strain.

PACS numbers: 62.20.de

*jgberryman@lbl.gov

I. INTRODUCTION

For both scientific and engineering purposes, researchers need to be able to characterize the mechanical behavior of the very great variety of natural and industrial polycrystalline solid media of either newly developed or continuing interest. Analysis of such polycrystalline aggregates usually proceeds by assuming (for practical reasons related to lack of detailed knowledge of the materials' internal arrangements) that the anisotropic crystals composing them are randomly oriented in space, so the overall average behavior can be well-approximated by isotropic effective bulk and shear moduli. Voigt and Reuss [1,2] estimates of these elastic constants came first to be followed later by Hill's discovery [3] that these same estimates were in fact rigorous — though often quite crude — bounds on the effective isotropic bulk and shear moduli. These relatively simple bounds have been frequently applied, especially (and most extensively) in tabulations for aggregates of cubic crystals [4-6].

Hashin-Shtrikman [7] bounds were developed later, using new variational principles, for improved bounds on elastic constants of polycrystalline solids — at first specifically again for those having cubic elastic symmetry. These variational methods were then generalized and applied later in a long series of papers directed towards providing improved rigorous bounds for many of the most important crystal symmetry classes [8-15]. However, all these results must nevertheless be used with some caution, because it is known that for electical conductivity and for bulk modulus there are results for special microstructures [16-19] that produce overall constants equaling, respectively, the upper Weiner [20] bound for the electrical conductivity, and either the computed Voigt (upper) or Reuss (lower) bounding values for the bulk modulus. So these special cases necessarily violate the Hashin-Shtrikman

bounds.

Kröner [21,22] showed that when some detailed statistical information is available for use in computing estimates of these constants, then a sequence of increasingly more sophisticated bounds could be constructed. Furthermore, the well-known self-consistent estimates were shown to coincide with the effective elastic moduli of perfectly (*i.e.*, maximally) disordered systems. Therefore, Kröner's work provides one interpretation of such self-consistent results based specifically on a polycrystalline microstructural characterization.

It follows that some knowledge of (which then provides some constraints on) the aggregate microstructure is essential to attaining truly rigorous improved (*i.e.*, better than the Voigt and Reuss) bounds. This fact explains in part why, when such microstructural information is lacking (as it very often is), that the main *estimates* still used in common practice for polycrystals are the typical Voigt-Reuss-Hill arithmetic averages [4-6], as suggested originally by Hill [3].

One question that naturally arises is whether there are better estimates currently available, perhaps using the information contained in the improved bounds themselves, when some microstructural information is actually known. A successful approach taken for this bounding problem has been based on detailed scans of the microstructure of polycrystals and subsequent computations based on measured [23] two-point and/or three-point spatial correlation functions by Beran [24] and Beran *et al.* [25]. More recently, still better estimates have been obtained using microtomographic imaging methods by Arns *et al.* [26].

Another approach to finding estimates of polycrystal bulk and shear moduli is the main subject of the present work. We show specifically how to obtain the so-called "self-consistent estimates," which are necessarily also consistent with (*i.e.*, lying within) the Hashin-Shtrikman bounds (because of the manner in which they are being constructed) for

the case of assumed spherical grain shapes. For other grain shapes and especially for assemblages involving multiple grain shapes, this analysis can in principle be repeated making use of earlier related work of Eshelby [27], Hill [28], Peselnick and Meister [8,9], Gubernatis and Krumhansl [29], Willis [30], Watt and Peselnick [10], and Watt [11-14], But discussion is limited here mostly to polycrystals formed from spherical crystals of $MgSiO_3$, since this is an especially important material for understanding elastic and seismic responses of the earth. Imposing the spherical shape condition also helps to exclude the issue previously mentioned about special microstructures that might achieve either the Voigt or Reuss bounds, since the spherical shapes are known to be excluded from those special cases.

There have also been many other preceding efforts to obtain self-consistent estimates as well as bounds for the elastic constants of polycrystals by (among others) Kröner [21, 22], Gubernatis and Krumhansl [29], Willis [30], Olson and Avellaneda [31], and Middya and Basu [32].

Related work of the author [33, 34] has treated a number of common materials with a wide range of anisotropic crystal structures. In contrast, the present contribution will concentrate on showing how the one common chemical compound $MgSiO_3$ (and analogs thereof) can result in a wide variety of elastic responses at different pressures and densities. Of all the various known approaches, the one that is perhaps the closest in spirit to the work presented here is that of Willis [30]. Some details of Willis's analysis were reviewed briefly [33], together with a discussion of relationships between Willis' work and that of Olson and Avellaneda [31]. The relationships to polycrystalline mechanics of orthotropic materials have also been treated recently [34].

Self-consistent estimation of effective elastic constants can be based instead on elastic wave scattering theory as was demonstrated by Gubernatis and Krumhansl [29], who derived

a set of self-consistent formulas valid for general crystal symmetry. See [34] for further discussion of such relationships.

In overview, the second (*i.e.*, next) section presents the stress-strain relations for two of the nine $MgSiO_3$ examples being considered here.

The third section gives details of our formulation (based mainly on Watt's work) for the trigonal and tetragonal cases treated here. This third section makes use of the results of two Appendices to reformulate the Peselnick-Meister-Watt (PMW) bounds and arrive at some useful analytical formulas for them.

The fourth section uses these formulas as a basis to construct one type of self-consistent estimate for random polycrystals, while the fifth section then presents some examples making use of both bounds and estimates, including additional results for the $CaIrO_3$ low-pressure analogs of the $MgSiO_3$ orthorhombics. Finally, the sixth section provides an overview of these results.

A very short review of the history of some pertinent technical aspects of this topic is provided here in Appendices A and B. Included are the known bounds of Voigt [1] and Reuss [2], as well as the pertinent Hashin-Shtrikman (HS) bounds and Peselnick-Meister-Watt (PMW) bounds (Hashin and Shtrikman [7], Peselnick and Meister [8], Meister and Peselnick [9], and Watt and Peselnick [10]), all of which are based on these Hashin-Shtrikman variational principles.

Recommended background reading includes the textbooks by Nye [35] (quick introduction to all the symmetry types to be considered in elastic analysis), Landau and Lifshitz [36] (various special topics in elasticity of particular interest to physicists), and Ting [37] (thorough discussion of symmetry types including extended discussion of the least symmetric types of elastic symmetry).

Results obtained show that — to the extent that random orientation of anisotropic crystals actually produces observable isotropic behavior — the Hashin-Shtrikman bounds fit tightly around the self-consistent estimates for all the $MgSiO_3$ polymorphs considered. These polymorphs are also all the ones currently known for $MgSiO_3$, including the recently discovered post-perovskite polymorph. The same general observations hold as well for the related $CaIrO_3$ analogs.

II. STRESS-STRAIN RELATIONS FOR TWO OF THE CRYSTAL SYMMETRY CLASSES: TRIGONAL ILMENITE AND TETRAGONAL MAJORITE

Members of the class of crystal symmetries considered first have their stress-strain relations given in one of three standard Voigt forms:

For ilmenite, $MgSiO_3$ has the trigonal (7 constant) structure, implying seven independent elastic constants following the general form:

$$\begin{pmatrix} \sigma_{11} \\ \sigma_{22} \\ \sigma_{33} \\ \sigma_{23} \\ \sigma_{31} \\ \sigma_{12} \end{pmatrix} = \begin{pmatrix} c_{11} & c_{12} & c_{13} & c_{14} & -c_{25} & \\ c_{12} & c_{11} & c_{13} & -c_{14} & c_{25} & \\ c_{13} & c_{13} & c_{33} & & & \\ c_{14} & -c_{14} & & c_{44} & & 2c_{25} \\ -c_{25} & c_{25} & & & c_{44} & 2c_{14} \\ & & & 2c_{25} & 2c_{14} & c_{66} \end{pmatrix} \begin{pmatrix} e_{11} \\ e_{22} \\ e_{33} \\ e_{23} \\ e_{31} \\ e_{12} \end{pmatrix}, \tag{1}$$

where σ_{ij} are the usual stress components for $i, j = 1 - 3$ in Cartesian coordinates, with 3 (or z) being the axis of symmetry, and $c_{66} = (c_{11} - c_{12})/2$. Displacement u_i is then related to strain component e_{ij} by $e_{ij} = \partial u_i/\partial x_j + \partial u_j/\partial x_i$, when $i \neq j$, and $e_{ii} = \partial u_i/\partial x_i$ when $i = j$.

Similarly, for the tetragonal (7 constant) majorite example, we have

$$\begin{pmatrix} \sigma_{11} \\ \sigma_{22} \\ \sigma_{33} \\ \sigma_{23} \\ \sigma_{31} \\ \sigma_{12} \end{pmatrix} = \begin{pmatrix} c_{11} & c_{12} & c_{13} & & & c_{16} \\ c_{12} & c_{11} & c_{13} & & & -c_{16} \\ c_{13} & c_{13} & c_{33} & & & \\ & & & c_{44} & & \\ & & & & c_{44} & \\ c_{16} & -c_{16} & & & & c_{66} \end{pmatrix} \begin{pmatrix} e_{11} \\ e_{22} \\ e_{33} \\ e_{23} \\ e_{31} \\ e_{12} \end{pmatrix} . \tag{2}$$

The count on elastic constants present in (1) and (2) shows there are seven independent ones in each. The distinct cases of trigonal (6 constants) and tetragonal (6 constants), already considered in earlier work [33], occur when $c_{25} = 0$ for trigonal, or $c_{16} = 0$ for tetragonal symmetry. See Nye [35] for a detailed discussion. The specific cases considered having these symmetries are ilmenite (trigonal) and majorite (tetragonal).

III. ELASTIC CONSTANT BOUNDS FOR RANDOM POLYCRYSTALS

The simplest elastic form to explain (but a hard case to compute) is for orthorhombic symmetry, which has nine independent elastic constants: c_{11}, c_{22}, c_{33}, c_{44}, c_{55}, c_{66}, c_{12}, c_{23}, c_{31}, together with the expected symmetric behavior of the off-diagonal components of all elastic materials. Orthorhombic symmetry applies to $MgSiO_3$ enstatite, protoenstatite, perovskite, and post-perovskite, and also to the $CaIrO_3$ post-perovskite and perovskite analogs considered. Methods used to treat these orthorhombic cases were presented earlier by the author [34], and briefly summarized here in Appendices A and B.

Voigt [1] and Reuss [2] estimates (shown to be upper and lower bounds respectively by Hill [3]) for the three crystal symmetry classes studied in this paper are reviewed in Appendix A. These bounds (in Appendix A) also help to motivate a pair of product formulas [33] that

are used repeatedly in the following discussion.

A. SIMPLIFIED BOUNDS ON BULK MODULUS

Known formulas [7] for the Hashin-Shtrikman-type bounds on polycrystals of grains having trigonal and tetragonal symmetries are reviewed in Appendix B. These bounds were derived originally by Peselnick and Meister [8] and Meister and Peselnick [9] with some corrections appended later by Watt and Peselnick [10]. The presentation of these bounds has been fairly complex, and so we will describe them as being expressed "algorithmically" – rather than as formulas. What we intend to imply by this statement is that the usual manner of presenting the results is sufficiently opaque that it is not immediately obvious how such bounds can be used to produce – for example – a set of self-consistent effective medium approximations based upon them.

Nevertheless, the two most common approaches for developing self-consistent estimates treat either (a) inclusions in a host medium, or (b) an aggregate composed entirely of anisotropic inclusions. A discussion of the earlier work of Willis [30] and its relationship to the Hashin-Shtrikman variational principle, as well as to a elasticity self-consistency condition was presented previously in earlier published work [33], and need not be repeated here.

To gain some useful insight towards deducing (in an operational sense) effective medium approximations based on rigorous bounds, it is helpful to have analytical formulas. Self-consistency formulas normally require the equivalent of an analytic continuation of some formula (or, in elasticity, a set of coupled formulas for bulk and shear moduli) in order to arrive at a practical approximation. One necessary step is to find appropriate analytic formulas for both bulk and shear moduli that can be used for these purposes.

A brief synopsis of the resulting analysis follows: The main technical machinery used in the construction of the actual Hashin-Shtrikman-type bounds is a certain matrix R having the necessary property that it is either positive definite or negative definite for isotropic comparison materials that bound the actual statistically isotropic effective constants for a random polycrystal. Conditions of positive or negative definiteness result in bounds on the principal minors of the comparison matrix R. These minors can then be parameterized in terms of the shear and bulk moduli $G_{\pm}$ and $K_{\pm}$ of the appropriate isotropic comparison material.

For whichever bounding method is being used, we then take the pair of comparison values G_{+}, K_{+} to be the best ones available for upper bounds, while G_{-}, K_{-} are similarly the best ones for the lower bounds. This designation implies that these particular comparison values give the tightest bounds possible without violating any of the known restrictions (*i.e.*, positive or negative definiteness) on the principal minors of R. But we may nevertheless choose (for operational simplicity) to evaluate the bounds at valid boundary points off the optimum values when it is most convenient to do so. Then, the key trial comparison values appearing in the Peselnick-Meister bounds are [for example, see Appendix B and (59)]

$$\beta_{\pm} \equiv -\frac{1}{5}\left[\frac{1}{G_{\pm}} + \frac{2}{3K_{\pm} + 4G_{\pm}}\right]. \tag{3}$$

The main algebraic observation that helps us to find simplified analytic formulas in this case is then based on the easily verified facts that

$$1 + 2\beta_{\pm}G_{\pm} = -2\beta_{\pm}\zeta_{\pm}, \tag{4}$$

where the derived parameters $\zeta_{\pm}$ are defined by

$$\zeta_{\pm} = \frac{G_{\pm}}{6}\left(\frac{9K_{\pm} + 8G_{\pm}}{K_{\pm} + 2G_{\pm}}\right). \tag{5}$$

In (5), the values of $G_\pm$ and $K_\pm$ are those defined algorithmically in Appendix B, using Eqs. (63)–(67). These values are related to parameters in Eshelby's well-known analysis [27] of elastic composites having ellipsoidal inclusions.

As one especially simple example, consider hexagonal symmetry: For the values in (5) and Appendix B, we might have $G_- = c_{44}$ and $G_+ = c_{66}$ (assuming for purposes of illustration that $c_{44} \leq c_{66}$, and that the other pertinent constants lie somewhere within this range). Then, the comparison values $K_\pm$ are given explicitly by

$$K_\pm = \frac{K_V(G^r_{\text{eff}} - G_\pm)}{(G^v_{\text{eff}} - G_\pm)}, \tag{6}$$

where G^v_{eff} (G^r_{eff}) is the "uniaxial shear energy" per unit volume for a unit applied shear strain (stress) whose main compressive strain (stress) is applied to the grains along their axis of symmetry. A definition of the term "uniaxial shear" is given following (33) in Appendix A. Also see [33] for extended discussion.

To obtain the desired results for bulk modulus, we now rearrange the Peselnick-Meister bounding form (57) [from Appendix A] into the formula

$$K^\pm_{PM} = \frac{K_V + K_\pm 2\beta_\pm(G_\pm - G^v_{\text{eff}})}{1 + 2\beta_\pm(G_\pm - G^v_{\text{eff}})}. \tag{7}$$

Then, using (6) [or see (63) in Appendix B], we have

$$K^\pm_{PM} = \frac{K_V[1 + 2\beta_\pm(G_\pm - G^r_{\text{eff}})]}{1 + 2\beta_\pm(G_\pm - G^v_{\text{eff}})}. \tag{8}$$

And, finally, substituting (4) into (8), we obtain one of the desired results:

$$K^\pm_{PM} = \frac{K_V(G^r_{\text{eff}} + \zeta_\pm)}{(G^v_{\text{eff}} + \zeta_\pm)}. \tag{9}$$

These formulas are simplified versions of the Peselnick-Meister-Watt (PMW) bounds on the overall bulk modulus, which are rigorous bounds derived from the Hashin-Shtrikman

variational principles for random polycrystals. Then, exactly the same formulas bounding bulk modulus are valid for two more symmetry classes considered here (*i.e.*, trigonal and tetragonal). Note that, for cubic symmetry [7], $K_V = K_R$ also implies $G^r_{\rm eff} = G^v_{\rm eff} = \mu_3 = \frac{1}{2}(c_{11} - c_{12})$, and so degenerates to $K^{\pm}_{PM} \equiv K_V$, as it clearly should.

The functional $\zeta(G_\pm, K_\pm) \equiv \zeta_\pm$ defined by (5) is demonstrably monotonic in both arguments $G_\pm$ and $K_\pm$. As $K_\pm$ ranges from 0 to ∞ for fixed $G_\pm$, $\zeta_\pm$ lies in the bounded range $\frac{2}{3}G_\pm \le \zeta_\pm \le \frac{3}{2}G_\pm$. As $G_\pm$ varies from 0 to ∞, $\zeta_\pm$ also ranges from 0 to ∞. In particular, when $\zeta_- = 0$, (9) shows that

$$K^-_{PM} = K_R, \tag{10}$$

which follows from the product formula $K_V G^r_{\rm eff}/G^v_{\rm eff} = K_R$. When $\zeta_+ = \infty$, (9) shows that

$$K^+_{PM} = K_V. \tag{11}$$

These two expressions are obviously lower and upper bounds on K as given by Reuss and Voigt, respectively. Thus, the analytical formula in (9) parameterizes the bounds on K in terms of the factors $\zeta_\pm$, which are both still determined by the formulas given for $G_\pm$ and $K_\pm$ in Appendix B. But, as will again be shown, the formula (9) has the advantage that it is also comparatively easy to use as the basis for a self-consistent effective medium approximation.

B. SIMPLIFIED BOUNDS ON SHEAR MODULUS

To find the simplified version of the Peselnick-Meister bounds for the overall shear modulus given by

$$\mu^{\pm}_{PM} = G_\pm + \frac{B^{\pm}_2}{1 + 2\beta_\pm B^{\pm}_2}, \tag{12}$$

with $B^{\pm}_2$ defined in (60) and (62) for the two symmetry classes considered, we first shift $G_\pm$ to the left hand side. Then multiply by $-2\beta_\pm$, and finally add unity to both sides, giving

the result:

$$\left[1 + 2\beta_{\pm}(G_{\pm} - \mu_{PM}^{\pm})\right] = \frac{1}{1 + 2\beta_{\pm}B_2^{\pm}}. \tag{13}$$

Using (4) to simplify the left hand side, we then have

$$\mu_{PM}^{\pm} + \zeta_{\pm} = -\frac{1}{2\beta_{\pm}(1 + 2\beta_{\pm}B_2^{\pm})}. \tag{14}$$

The right hand side of (14) can be greatly simplified for all the symmetry classes considered here, but unlike the bulk modulus [see (9)], the resulting formulas for shear modulus are distinct — *i.e.*, they depend on the symmetry class.

To illustrate these ideas, first consider the simpler case of hexagonal symmetry. When some work (*i.e.*, rather tedious algebra) has been completed for this case, the formula (14) can be inverted to give

$$\frac{1}{\mu_{\rm hex}^{\pm} + \zeta_{\pm}} = \frac{1}{5}\left[\frac{1 - \alpha_{\pm}(K_V - K_{\pm})}{G_{\rm eff}^{v} + \zeta_{\pm} + \frac{\alpha_{\pm}}{2\beta_{\pm}}(K_V - K_{\pm})} + \frac{2}{c_{44} + \zeta_{\pm}} + \frac{2}{c_{66} + \zeta_{\pm}}\right], \tag{15}$$

where the factors $\alpha_{\pm}$ are defined in (59) of Appendix B.

For *hexagonal symmetry*, the formulas in (15) reduce correctly to (31) as $\zeta_+ \to \infty$ and to (35) as $\zeta_- \to 0$, *i.e.*, becoming respectively the Voigt and Reuss bounds on the polycrystal's overall shear modulus. The result for $\zeta_+ \to \infty$ [which also implies $K_+ \to K_V$ using (9)] is obtained from a standard limiting process. Some intermediate steps in the $\zeta_- \to 0$ calculation are: $K_- \to K_R$, $\alpha_- \to -1/K_R$, and $\beta_- \to \infty$. The expected Reuss result (35) is then obtained, because $K_V/G_{\rm eff}^{v}K_R = 1/G_{\rm eff}^{r}$ follows from some known product formulas [33]. Terms identical to the complicated first one here on the right hand side appear in formulas for all these symmetry classes. The form of these shear modulus bounds cannot be simplified further because the Voigt and Reuss bounds depend on the (usually distinct) factors $G_{\rm eff}^{v}$ and $G_{\rm eff}^{r}$, respectively. These terms provide an essential link (which we may view as an interpolation formula) between these limits.

When the analogous steps are carried through for *trigonal symmetry*, we find:

$$\frac{1}{\mu^{\pm}_{\rm trig}+\zeta_{\pm}} = \frac{1}{5}\left[\frac{1-\alpha_{\pm}(K_V-K_{\pm})}{G^{v}_{\rm eff}+\zeta_{\pm}+\frac{\alpha_{\pm}}{2\beta_{\pm}}(K_V-K_{\pm})}+\frac{2}{\mu^{tr}_{1}+\zeta_{\pm}}+\frac{2}{\mu^{tr}_{2}+\zeta_{\pm}}\right], \tag{16}$$

where μ^{tr}_1 and μ^{tr}_2 are defined later in equations (39) and (40) of Appendix A.

For *tetragonal symmetry*, we find similarly that:

$$\frac{1}{\mu^{\pm}_{\rm tetr}+\zeta_{\pm}} = \frac{1}{5}\left[\frac{1-\alpha_{\pm}(K_V-K_{\pm})}{G^{v}_{\rm eff}+\zeta_{\pm}+\frac{\alpha_{\pm}}{2\beta_{\pm}}(K_V-K_{\pm})}+\frac{1}{\mu_{3}+\zeta_{\pm}}+\frac{2}{c_{44}+\zeta_{\pm}}+\frac{1}{c_{66}+\zeta_{\pm}}\right], \tag{17}$$

where

$$\mu_3 \equiv (c_{11}-c_{12})/2, \tag{18}$$

and μ^{te}_1 and μ^{te}_2 are defined in equations (52) and (53) of Appendix A. Note that, if $\mu_3 \equiv c_{66}$ (as is true for the trigonal case under consideration here), then (17) would be formally the same as (15). But these results remain distinct since this condition does not hold for any of the tetragonal problems being considered.

Cubic symmetry (although our main interests here are instead orthorhombic, trigonal, and tetragonal symmetries) requires $c_{11}=c_{22}=c_{33}$, $c_{12}=c_{13}=c_{23}$, $c_{44}=c_{55}=c_{66}$. This symmetry class may therefore be viewed as a special case of the tetragonal symmetry class. As such, we can immediately write the results for the bounds. It was already noted that $K^{\pm}_{PM}=K_{\pm}\equiv K_V$ for cubic symmetry. Then, $G^{v}_{\rm eff}=G^{r}_{\rm eff}=\mu_3=\frac{1}{2}(c_{11}-c_{12})$. So (17) for cubic symmetry becomes

$$\frac{1}{\mu^{\pm}_{\rm cub}+\zeta_{\pm}} = \frac{1}{5}\left[\frac{2}{G^{v}_{\rm eff}+\zeta_{\pm}}+\frac{3}{c_{44}+\zeta_{\pm}}\right]. \tag{19}$$

The bounds in (19) are identical to those originally found by Hashin and Shtrikman [7] — also see Willis [30] — for this case. But the displayed form is more symmetrical than those usually presented, helping to emphasize the role of the eigenvalues themselves, as well as

their multiplicity. Thus, (19) establishes a useful analogy between formulas for cubic and tetragonal symmetry.

The uniaxial shear energies $G^v_{\rm eff}$ and $G^r_{\rm eff}$, as defined in Appendix A, play a key role (and essentially the same role for all these symmetry types) in these formulas even though they are seldom simply related to true eigenvalues of the equations of elasticity.

IV. SELF-CONSISTENT ESTIMATES OBTAINED FROM THE BOUNDS

We are now ready to create some useful effective medium approximations based on the formulas for the rigorous bounds (9) and (15)-(19) derived in the previous section. In each case, the choices made seem obvious based both on the form of these bounds, and on prior experiences with other bounds and self-consistent estimates [34]. The resulting formulas obtained this way will be called the "self-consistent" or SC estimates based on these bounds obtained via the Hashin-Shtrikman variational principles. A review of some earlier self-consistency results for this same class of problems is presented in Appendix B.

These results can be written in several different forms. The self-consistent estimate for bulk modulus may, for example, be chosen as

$$K^* = \frac{K_V(G^r_{\rm eff}+\zeta^*)}{(G^v_{\rm eff}+\zeta^*)} = \frac{(G^v_{\rm eff}K_R+\zeta^* K_V)}{(G^v_{\rm eff}+\zeta^*)}, \tag{20}$$

where

$$\zeta^* = \frac{\mu^*}{6}\left(\frac{9K^*+8\mu^*}{K^*+2\mu^*}\right). \tag{21}$$

In (21), K^* is determined by (20), depending on μ^*. The value of μ^* is itself determined by the self-consistent expression for the shear modulus to follow, depending on K^*; and parameter ζ^* is determined by (21). The general formulas (20) and (21) are true for all three symmetry classes, but the final results will *differ by symmetry class* because of the

various distinct formulas for μ^* that follow.

In the course of the derivation of the bounds by Watt and Peselnick [10], the authors show that there are some terms that appear of the form

$$\frac{1}{3}\beta_{\pm}\Delta = 2\beta_{\pm}\left[K_V\left(G^r_{\text{eff}} - G_{\pm}\right) - K_{\pm}\left(G^v_{\text{eff}} - G_{\pm}\right)\right]. \tag{22}$$

[Compare equation (61) in Appendix B.] It follows immediately from the constraint equations in (63) that this expression vanishes identically *for their algorithmic expression of the bounds*. However, when we move off of these constraint curves in order to find the self-consistent expressions (thus, decoupling $K_{\pm}$ and $G_{\pm}$), this expression no longer vanishes and we need to be careful to include its effect in the formulas for the self-consistent shear modulus. Again making use of the identity (4), we find easily that

$$\frac{1}{3}\beta^*\Delta = K_V - K^* + 2\beta^*\left[K_V\left(G^r_{\text{eff}} + \zeta^*\right) - K^*\left(G^v_{\text{eff}} + \zeta^*\right)\right]. \tag{23}$$

Now, the expression for the self-consistent bulk modulus K^* in (20) shows that most of the terms in this expression sum to zero. So the final result reduces to

$$\frac{1}{3}\beta^*\Delta = K_V - K^*. \tag{24}$$

For the self-consistency conditions we seek, this term is multiplied by α^* and then added to the denominator of the term also containing a factor of $G^v_{\text{eff}} + \zeta^*$. When these steps are all accomplished, the result is in agreement with the results obtained by several other published methods of deriving self-consistent formulas, including Middya and Basu's contribution [32] for orthorhombic symmetry.

The end result for μ^* in polycrystals having grains with *hexagonal* symmetry is

$$\frac{1}{\mu^*_{\text{hex}} + \zeta^*} = \frac{1}{5}\left[\frac{1 - \alpha^*(K_V - K^*)}{G^v_{\text{eff}} + \zeta^*} + \frac{2}{c_{44} + \zeta^*} + \frac{2}{c_{66} + \zeta^*}\right]. \tag{25}$$

Then, for *trigonal* symmetry, (16) with the Δ correction needed for analytic continuation and self-consistency gives:

$$\frac{1}{\mu^*_{\rm trig}+\zeta^*}=\frac{1}{5}\left[\frac{1-\alpha^*(K_V-K^*)}{G^v_{\rm eff}+\zeta^*}+\frac{2}{\mu_1+\zeta^*}+\frac{2}{\mu_2+\zeta^*}\right]. \tag{26}$$

Finally, for *tetragonal* symmetry, we have from (17) with the required Δ correction:

$$\frac{1}{\mu^*_{\rm tetr}+\zeta^*}=\frac{1}{5}\left[\frac{1-\alpha^*(K_V-K^*)}{G^v_{\rm eff}+\zeta^*}+\frac{1}{\mu_3+\zeta^*}+\frac{2}{c_{44}+\zeta^*}+\frac{1}{c_{66}+\zeta^*}\right], \tag{27}$$

where μ_3 was defined in (18).

As pointed out previously, since cubic symmetry may be viewed as a special case of tetragonal symmetry, the self-consistent formulation for cubic symmetry does not require separate treatment. On the other hand, cubic symmetry is also probably the one case that has been studied most often by many authors, including Hashin and Shtrikman [7], Hill [28], and Willis [30]. Thus, cubic symmetry may deserve some special attention. Since $K_V = K_R = K^*$ for cubic crystals, the only self-consistent formula needed for this case is the one for shear modulus, which can be written either as

$$\frac{1}{\mu^*_{\rm cub}+\zeta^*}=\frac{1}{5}\left[\frac{2}{\mu_3+\zeta^*}+\frac{3}{c_{44}+\zeta^*}\right], \tag{28}$$

or in the form presented in (19) for the bounds. The result (28) follows directly from (27) since $\mu_3 = G^V_{\rm eff} = \frac{1}{2}(c_{11}-c_{12})$ and $c_{66} = c_{44}$ for cubic symmetry. Using the definition of ζ^* from (21), we also find easily that μ^* satisfies the cubic equation

$$8(\mu^*)^3+(9K+4\mu_3)(\mu^*)^2-3c_{44}(K+4\mu_3)\mu^*-6Kc_{44}\mu_3=0. \tag{29}$$

Equation (29) is exactly the same as the formula given by Willis [30] [p. 46] for the self-consistent shear modulus of a cubic system. The corresponding pair of equations for the upper and lower Hashin-Shtrikman bounds for a polycrystal having grains with cubic sym-

metry is also exactly the same as those quoted by Hashin and Shtrikman [7] and by Willis [30], but presented in a more symmetric and, therefore, perhaps more intuitive form in (28).

In all these cases, these self-consistent formulas may be obtained operationally by replacing terms in the bounds everywhere so that $K_\pm \to K^*$, $G_\pm \to \mu^*$, and $\zeta_\pm \to \zeta^*$. The single term in both shear modulus bounds and estimates that captures the contribution of the uniaxial shear mode must be treated with extra care, since the term in the denominator proportional to $\frac{1}{3}\beta_\pm\Delta$ vanishes identically for the bounds, but $\frac{1}{3}\beta^*\Delta$ does not vanish for the self-consistent estimates. After making this correction, the resulting formula for these estimates is in complete agreement with that of other derivations. The final result is a set of coupled equations that are most conveniently solved by numerical iteration.

The resulting iteration scheme is expected (and generally found in practice) to converge rapidly to definite unique positive values for both K^* and μ^*, and the convergence is especially quick when it can be shown that the individual formulas are monotonic functionals of their arguments. It is well-known that $\zeta^* = \zeta(\mu^*, K^*)$ is a monotonic functional of both arguments. It is also quite easy to check using (20) that K^* is a monotonic functional of ζ^*. Since $K^* \leq K_V$ will always be satisfied, μ^* is easily shown for all three crystal symmetries considered to be a monotonic functional of ζ^*.

The only remaining constraint that should be checked is whether μ^* is also a monotonic functional of K^*. This analysis (being easy enough to do that it will not be shown here) indicates that μ^* is indeed a monotonic functional of K^*. Numerical examples computed show that convergence is very quick in almost all cases. For comparison purposes, we display the values of G^v_{eff} in all the following examples, since this parameter is key to the analytic properties of both the bounds and estimates.

V. EXAMPLES

There are nine specific examples of $MgSiO_3$ behavior presented in the first six TABLES. Of these nine examples, the higher pressure results are plotted in the first two Figures. For comparison purposes, four examples of results for $CaIrO_3$ post-perovskite and perovskite (low-pressure analogs of $MgSiO_3$ systems) are also presented here in TABLES 7 and 8, and in Figs. 3 and 4. Then all nine examples of $MgSiO_3$ are then replotted together in the curves contained in Fig. 5.

As one quantitative check on our results, we may compare the values for $MgSiO_3$ trigonal (7 constant) ilmenite obtained by Watt [13] with those obtained here. Watt's computed values (in GPa) are: $K_{HS}^- = 211.1$, $K_{HS}^+ = 212.5$, $G_{HS}^- = 131.0$, and $G_{HS}^+ = 134.2$, while the corresponding values obtained here are: $K_{HS}^- = 211.2$, $K_{HS}^+ = 213.0$, $G_{HS}^- = 131.0$, and $G_{HS}^+ = 135.2$. Watt quotes the same reference for the original ilmenite data as was used here, so any discrepancies presumably should be attributed to the fact that Watt used a search routine to evaluate the optimum bounds, and we have chosen to skip this step, as the improvements in the results are usually not large (typically less than 1%). Corresponding values are nevertheless seen to be quite close for this case.

Similarly, for orthotropic enstatite, Watt [11] finds: $K_{HS}^- = 107.8$, $K_{HS}^+ = 107.8$, $G_{HS}^- = 75.6$, $G_{HS}^+ = 75.7$, while our corresponding values obtained here are: $K_{HS}^- = 107.7$, $K_{HS}^+ = 107.8$, $G_{HS}^- = 75.5$, $G_{HS}^+ = 75.7$ – together with $K_{SC} = 107.8$ and $G_{SC} = 75.7$. Bass [6] and Watt [11] both quote the same source for the crystal data [39]. Differences again are very small, and most likely should be attributed to differences between Watt's search routine, and the method used here without making use of such a search routine for orthotropic symmetry.

In all of the first four Figures, the rectangles forming the Voigt-Reuss bounds and the

Hashin-Shtrikman bounds are shown in black and blue, respectively. When the Hashin-Shtrikman bounding rectangle is hard to see in these Figs., this situation results from the fact that the HS bounds are fitting very tightly around the self-consistent point estimate, which is itself indicated by a red asterisk. The VRH (Voigt-Reuss-Hill) point is shown as a green plus sign, and this point is always exactly in the middle of VR rectangle. The geometric mean point on these plots is exactly at the center of the small black diamond. In general, we find that the VRH and GM estimates are very close to each other for the orthorhombic examples computed here, although this is not necessarily a general rule for all materials and all elastic symmetries.

The numerical implementation of the formulas for orthorhombic symmetry were discussed in more detail in Ref. [34].

Note that the data being used here have been quoted without specifying measurement uncertainty. Clearly, knowledge of the single-crystal data uncertainty and error propagation through the formulas presented is an important reality check.

VI. DISCUSSION AND CONCLUSIONS

As we have seen in the discussion of the examples, the chemical compound $MgSiO_3$ is very common in the earth, and comes in many forms including a variety of crystal symmetries. One form of $MgSiO_3$ is a perovskite, which presents one orthorhombic form (having 9 independent elastic constants) of this crystalline compound. There are also two pyroxenes, namely enstatite and protoenstatite, that are based on two more distinct (also 9 constant) orthorhombic forms. The material is found as well in the ilmenite structure which has trigonal (7 constant) elastic symmetry, as well as the majorite structure which has tetragonal (7 elastic constant) symmetry with the garnet structure. The comparatively recently discov-

ered post-perovskite form also possesses orthorhombic symmetry, as does perovskite itself. Analysis presented here concentrated on computing effective isotropic polycrystal constants – *i.e.*, bulk and shear moduli – for random aggregates of each of these forms. In order to compare and contrast these results, the observable trends among these behaviors have been quantified – as a function of confining pressure, and therefore density. Results show that effective bulk modulus increases by a factor of about six, while the shear modulus increases only by a factor of about three, as the aggregate density changes by a factor of a little less than two. Results for related $CaIrO_3$ analogs of $MgSiO_3$ also show qualitatively very similar elastic constant behavior.

Our final Figure 5 illustrates the general trends in these examples such that bulk and shear moduli generally increase as the applied pressure and corresponding density of the material both increase. The shear modulus appears to be very nearly a linear function of density ρ, to a good first approximation. Bulk modulus shows a more complicated S-shaped behavior, increasing at a slower rate with increasing density for lower density, and then a steady transition to distinctly higher values above $\rho = 5.0$ Mg/m^3. Shear modulus has increased by about a factor of three, while the bulk modulus has increased by a factor of six. So bulk modulus is about twice as sensitive to density increases as shear modulus. The density itself has increased by a factor of about 1.8 in these examples.

Two early papers [51, 52] that should be mentioned emphasize optimality conditions on bulk and shear modulus behavior for some special microgeometries such as multi-layered laminates or planar geometries (such as thin films). These papers have provided complete characterizations of bulk and shear modulus bounds for some precisely specified microstructures. Such work can provide useful information within the specified contexts, but differs in both thrust and scope from the work presented here which in contrast has concentrated

instead on random three-dimensional polycrystals. We expect many real earth systems that have developed over geologic time will be better represented by such inherently random models.

To sum up: The focus of the present effort has differed from that of most previous studies of polycrystal elasticity. We have concentrated our attention mostly on a single chemical compound ($MgSiO_3$), which is believed to be the most common constituent of the earth's interior. It occurs in six distinct forms (*i.e.*, having six different crystal symmetries). This situation provides a unique opportunity to understand and also quantitatively characterize interrelationships among pressure, elastic response (*i.e.*, in the form of the effective bulk and shear moduli), and related issues such as morphing of preferred crystal symmetry with large increases in confining pressure. The advantage of this treatment becomes most apparent through the reduction of variable count (from as many as nine distinct elastic constants for orthorhombic symmetry) to only the two effective moduli for the overall average bulk and shear behavior. These two curves can then be conveniently plotted together on the same 2D plot versus pressure as illustrated in Fig. 5.

APPENDIX A: Product Formula in Elasticity Related to Voigt and Reuss Bounds

Based on earlier work [24-30], the author has treated in Ref. [33] the simpler cases of hexagonal symmetry, trigonal symmetry (6 constants), and tetragonal symmetry (6 constants). Behavior of pure materials involving only cubic symmetry is sufficiently simple to analyze that it can actually be treated as a special case of hexagonal symmetry, and therefore does not require separate treatment. We do not treat either cubic or hexagonal symmetry directly in the present paper. Nevertheless, it is helpful to explain some of the concepts used here by first defining symbols for some combinations of the elastic parameters that occur

repeatedly.

The more difficult examples that we do treat are the cases of trigonal (7 constants), and tetragonal (7 constants) symmetries. These cases have already been studied previously by Watt [13], and we borrow heavily from this published work. We also make use of recent work on orthorhombic symmetry [34], but do not elaborate on the details of that analysis again here.

Voigt averages

The Voigt average for bulk modulus of a trigonal system (having either 6 or 7 constants) is given by:

$$K_V = [2(c_{11} + c_{12}) + c_{33} + 4c_{13}]/9. \tag{30}$$

Uniaxial Shear

A useful concept arising in earlier work is that of "uniaxial shear." To provide a simple example, consider a hexagonal system having the Voigt estimate μ_V for the upper bound on the effective shear modulus. This quantity can be written as

$$\mu_V = \frac{1}{5}\left(G^v_{\text{eff}} + 2c_{44} + 2c_{66}\right), \tag{31}$$

where the new term appearing here is defined by (31) and given explicitly by

$$G^v_{\text{eff}} = (c_{11} + c_{33} - 2c_{13} - c_{66})/3. \tag{32}$$

The quantity G^v_{eff} has the physical significance of being the energy per unit volume in a grain when a pure "uniaxial shear" *strain* of unit magnitude [*i.e.*, $(e_{11}, e_{22}, e_{33}) = (1, 1, -2)/\sqrt{6}$], whose main compressive strain is applied to the grain along its axis of symmetry [33].

The term "uniaxial shear" may therefore be used in the following sense: If a uniaxial principal stress (or strain) of three units is applied along the symmetry axis, then we have

$$\begin{pmatrix} 0 \\ 0 \\ 3 \\ 0 \\ 0 \\ 0 \end{pmatrix} = \begin{pmatrix} 1 \\ 1 \\ 1 \\ 0 \\ 0 \\ 0 \end{pmatrix} - \begin{pmatrix} 1 \\ 1 \\ -2 \\ 0 \\ 0 \\ 0 \end{pmatrix}. \tag{33}$$

The first vector on the right hand side is a pure compressional stress (or strain) and the second is clearly a pure shear stress (or strain). Therefore, on physical grounds, it seems reasonable to call the second vector on the right "the shear component of a uniaxial stress (or strain)," or the "uniaxial shear" for short — without needing to specify the stress or strain nature of the excitation, as this will normally be clear in this context.

Similarly, the Reuss average for bulk modulus of a system having hexagonal crystal symmetry is determined by $1/K_R = 2(s_{11} + s_{12}) + 4s_{13} + s_{33}$, which can also be written as

$$\frac{1}{K_R - c_{13}} = \frac{1}{c_{11} - c_{66} - c_{13}} + \frac{1}{c_{33} - c_{13}} \tag{34}$$

in terms of stiffness coefficients. The Reuss average for shear in this case is given by

$$\mu_R = \left[\frac{1}{5}\left(\frac{1}{G^r_{\text{eff}}} + \frac{2}{c_{44}} + \frac{2}{c_{66}}\right)\right]^{-1}, \tag{35}$$

which form may again be taken as the definition of G^r_{eff}. So it is the energy per unit volume in a grain when a pure uniaxial shear *stress* of unit magnitude [*i.e.*, $(\sigma_{11}, \sigma_{22}, \sigma_{33}) = (1, 1, -2)/\sqrt{6}$], whose main compressive pressure is applied to a grain along its axis of symmetry.

A useful product formula then arises as the formal definition of $G^r_{\rm eff}$: For each grain having hexagonal symmetry, two interrelated product formulas hold [33]: $3K_R G^v_{\rm eff} = 3K_V G^r_{\rm eff} = \omega_+\omega_-/2 = c_{33}(c_{11}-c_{66}) - c_{13}^2$. The symbols $\omega_\pm$ stand for the quasi-compressional and quasi-uniaxial-shear eigenvalues for the crystalline grains. Thus, $G^r_{\rm eff} = K_R G^v_{\rm eff}/K_V$ – which is a general formula that holds for all three of the crystal symmetry types that were originally treated in Ref. [33]. Then, we may consider (31) and (35) [or their equivalents for other symmetries] as the fundamental defining equations for $G^v_{\rm eff}$ and $G^r_{\rm eff}$, respectively. While this observation was not present in the various published works of Watt, it turns out that many of Watt's formulas can be greatly simplified if we make use of these definitions.

It turns out that we can also make use of these ideas in simplifying Watt's formulas for trigonal (7 constant) symmetry, and for tetragonal (7 constant) symmetry in the following analysis, as will be demonstrated next.

Trigonal (7 constant) symmetry

For trigonal symmetry — restricted to classses 3, $\bar{3}$ – see Nye [35] — the nonzero stiffness constants are: c_{11}, c_{12}, $c_{13} = c_{23}$, $c_{14} = c_{56} = -c_{24}$, c_{25}, c_{33}, $c_{44} = c_{55}$, and the restriction that $c_{66} = (c_{11} - c_{12})/2$. Using the concept already introduced, we can define

$$G^v_{eff} = (c_{11} + c_{12} + 2c_{33} - 4c_{13})/6, \tag{36}$$

which has the same interpretation given earlier in terms of an effective shear mode behavior. This combination of constants can be compared to Watt's constant $M = 6G^v_{eff}$ in this notation.

So, for trigonal symmetry, the Voigt averages for bulk and shear moduli are again given by (30) and (31). The Reuss average for bulk modulus can be expressed in terms of the

product formulas as

$$K_R = \frac{\omega_+\omega_-}{6G^v_{\text{eff}}}, \tag{37}$$

where G^v_{eff} is again given by (32). And we find that

$$\mu_R = \left[\frac{1}{5}\left(\frac{1}{G^r_{\text{eff}}} + \frac{2}{\mu_1} + \frac{2}{\mu_2}\right)\right]^{-1}, \tag{38}$$

where

$$\mu_1^{tr} = \frac{1}{2}\left[c_{44} + c_{66} - \left([c_{44} - c_{66}]^2 + 4c_{14}^2 + 4c_{25}^2\right)^{1/2}\right], \tag{39}$$

$$\mu_2^{tr} = \frac{1}{2}\left[c_{44} + c_{66} + \left([c_{44} - c_{66}]^2 + 4c_{14}^2 + 4c_{25}^2\right)^{1/2}\right], \tag{40}$$

and

$$G^r_{\text{eff}} = \frac{\omega_+\omega_-}{6K_V}. \tag{41}$$

It is instructive (and useful to the discussion in the main text) to note that (31) can also be written for trigonal symmetry as

$$\mu_V = \frac{1}{5}\left(G^v_{\text{eff}} + 2\mu_1^{tr} + 2\mu_2^{tr}\right). \tag{42}$$

Or, more commonly, we have

$$\mu_V = \frac{1}{5}\left(G^v_{\text{eff}} + 2c_{44} + 2c_{66}\right). \tag{43}$$

Using the definition $\mu_3 = (c_{11} - c_{12})/2$ from (18), we have the conditions determining the boundaries of the allowed elastic behavior of the system according to the Hashin-Shtrikman bounding methods for trigonal (7 constant) symmetry:

$$0 \leq G_0 \leq \min[c_{44}, c_{66}, \mu_1^{tr}, G^r_{eff}] \tag{44}$$

and

$$\max[c_{44}, c_{66}, \mu_2^{tr}, G^v_{eff}] \leq G_0 \leq \infty. \tag{45}$$

Tetragonal (7 constant) symmetry

For tetragonal symmetry — restricted to classses 4, $\bar{4}$, $4m$ (see Nye [35]) — the nonzero stiffness constants are: c_{11}, c_{12}, $c_{13} = c_{23}$, c_{16}, c_{33}, $c_{44} = c_{55}$, and c_{66} (which is not coupled to c_{11} and c_{12} as it was in the previous case).

For this example, the Voigt average for bulk modulus is again given by (30), while the Voigt average for shear modulus is given now by

$$\mu_V = \frac{1}{5}\left(G^v_{eff} + \mu_3 + 2c_{44} + c_{66}\right), \tag{46}$$

where again we have [as in (18)]

$$\mu_3 \equiv (c_{11} - c_{12})/2 \tag{47}$$

and

$$G^v_{\text{eff}} = \left(c_{11} + c_{12} - 4c_{13} + 2c_{33}\right)/6. \tag{48}$$

(Note that the formula specifying G^v_{eff} for trigonal symmetry could also have been written this way — but not vice versa.) The Reuss average for bulk modulus is again given by (37), using this definition of G^v_{eff}. Alternatively, we have

$$\frac{1}{K_R - c_{13}} = \frac{2}{c_{11} + c_{12} - 2c_{13}} + \frac{1}{c_{33} - c_{13}}, \tag{49}$$

a form which is also valid for hexagonal and trigonal symmetries, whereas (34) is not valid for tetragonal symmetry. The Reuss average for shear modulus is

$$\mu_R = \left[\frac{1}{5}\left(\frac{1}{G^r_{\text{eff}}} + \frac{1}{\mu_3} + \frac{2}{c_{44}} + \frac{1}{c_{66}}\right)\right]^{-1}, \tag{50}$$

where we again have

$$G^r_{\text{eff}} = \frac{\omega_+\omega_-}{6K_V}, \tag{51}$$

and where, for tetragonal symmetry, $\omega_+\omega_- = [(c_{11}+c_{12})c_{33} - 2c_{13}^2]$. The form of (46) should also be compared to that of (50).

For this application, it is also handy to make use of the following definitions [also compare (39) and (40)]:

$$\mu_1^{te} = \frac{1}{4}[(c_{11} - c_{12} + 2c_{66}) - ([c_{11} - c_{12} - 2c_{66}]^2 + 16c_{16}^2)^{1/2}] \tag{52}$$

and, similarly,

$$\mu_2^{te} = \frac{1}{4}[(c_{11} - c_{12} + 2c_{66}) + ([c_{11} - c_{12} - 2c_{66}]^2 + 16c_{16}^2)^{1/2}]. \tag{53}$$

Though less commonly observed, we also find that

$$\mu_V = \frac{1}{5}\left(G_{\text{eff}}^v + 2c_{44} + \mu_1^{te} + \mu_2^{te}\right). \tag{54}$$

Again, using the same definition for $\mu_3 = (c_{11} - c_{12})/2$ as in (18), we have the conditions determining the boundaries of the allowed elastic behavior of the system according to the Hashin-Shtrikman bounding methods for tetragonal (7 constant) symmetry:

$$0 \leq G_0 \leq \min[c_{44}, \mu_1^{te}, \mu_3, G_{eff}^r] \tag{55}$$

and

$$\max[c_{44}, \mu_3, \mu_2^{te}, G_{eff}^v] \leq G_0 \leq \infty. \tag{56}$$

These conditions are algorithmically similar for either trigonal (7 constants) or tetragonal (7 constants) symmetry, but are not identical. The μ^* expressions to be used in each case are respectively (39) and (40) for trigonal (7 constants) and (52) and (53) for tetragonal (7 constants). Operationally, the task involved is now to determine the optimum (tightest) set of bounds determined by the stated bounding conditions. To do so in principle therefore requires a search algorithm. In practice, we find that it is generally adequate for most

purposes simply to evaluate the min and max expressions, and use these quantities as the values determining our estimates of the bounds.

APPENDIX B: Hashin-Shtrikman-Watt Bounds for Trigonal (7) and Tetragonal (7) Symmetries and Self-Consistency Relations

Hashin-Shtrikman-style bounds [7, 10, 33] on the bulk and shear moduli of isotropic random polycrystals composed of trigonal (7 constants) and tetragonal (7 constants) grains have been derived by Watt [13]. We use a slightly modified notation here, taking into account the product formulas [33] — and our preceding Appendix A — in order to simplify the statement of results. Derivations are found in the references, and therefore will not be repeated here.

Parameters used to optimize the Hashin-Shtrikman bounds are $K_\pm$ and $G_\pm$, and have the significance of being the bulk and shear moduli of two ($\pm$) isotropic comparison materials. G_+, K_+ are the values used in the formulas for the upper bounds, and G_-, K_- for the lower bounds. Formulas for the bounds then take the form:

$$K_{HSW}^{\pm} = K_\pm + \frac{K_V - K_\pm}{1 + 2\beta_\pm(G_\pm - G_{\rm eff}^v)}, \tag{57}$$

and

$$\mu_{HSW}^{\pm} = G_\pm + \frac{B_2^\pm}{1 + 2\beta_\pm B_2^\pm}, \tag{58}$$

where

$$\alpha_\pm = \frac{-1}{K_\pm + 4G_\pm/3}, \qquad \beta_\pm = \frac{2\alpha_\pm}{15} - \frac{1}{5G_\pm}, \qquad \gamma_\pm = \frac{1}{9}(\alpha_\pm - 3\beta_\pm). \tag{59}$$

The specific form of $B_2^\pm$ depends on crystal symmetry.

For trigonal (7 constant) symmetry, we have

$$B_2^\pm = \frac{1}{5}\Big[\frac{G_{\rm eff}^v - G_\pm}{\mathcal{D}_\pm} + \frac{2(\mu_1^{tr} - G_\pm)}{1 - 2\beta_\pm(\mu_1^{tr} - G_\pm)} + \frac{2(\mu_2^{tr} - G_\pm)}{1 - 2\beta_\pm(\mu_2^{tr} - G_\pm)}\Big], \tag{60}$$

where $\mathcal{D}_\pm$ is defined as

$$\mathcal{D}_\pm = 1 - 2\beta_\pm(G^v_{eff} - G_\pm) - \alpha_\pm(K_V - K_\pm) + \frac{\alpha_\pm\beta_\pm}{3}\Delta. \tag{61}$$

while using the definitions of K_V and $G^v_{\rm eff}$ appropriate for the trigonal symmetry.

For tetragonal (7 constant) symmetry, we have

$$B_2^\pm = \frac{1}{5}\Big[\frac{G^v_{\rm eff} - G_\pm}{\mathcal{D}_\pm} + \frac{(\mu_3 - G_\pm)}{1 - 2\beta_\pm(\mu_3 - G_\pm)} + \frac{2(c_{44} - G_\pm)}{1 - 2\beta_\pm(c_{44} - G_\pm)} + \frac{(c_{66} - G_\pm)}{1 - 2\beta_\pm(c_{66} - G_\pm)}\Big], \tag{62}$$

where $\mathcal{D}_\pm$ is defined as in (61), but now using the definitions of K_V and $G^v_{\rm eff}$ appropriate for the tetragonal symmetry, with μ_3 defined in (18).

Optimum values of the moduli $K_\pm$ and $G_\pm$ for the comparison materials have been shown to be (in the present notation)

$$K_\pm = \frac{K_V(G^r_{\rm eff} - G_\pm)}{(G^v_{\rm eff} - G_\pm)}, \tag{63}$$

where, for K_-,

$$0 \le G_- \le \min(\mu_2, G^r_{\rm eff}) \qquad \text{(trigonal – 7 constants)}, \tag{64}$$

$$0 \le G_- \le \min(c_{44}, \mu_3, G^r_{\rm eff}, c_{66}) \qquad \text{(tetragonal – 7 constants)}, \tag{65}$$

and μ_3 defined in (18). Similarly, for the K_+ formula,

$$\max(G^v_{\rm eff}, \mu_1) \le G_+ \le \infty \qquad \text{(trigonal – 7 constants)}, \tag{66}$$

$$\max(c_{44}, \mu_3, G^v_{\rm eff}, c_{66}) \le G_+ \le \infty \qquad \text{(tetragonal – 7 constants)}, \tag{67}$$

Note that, when $G_- = 0$, $K_- = K_R$, because $K_R = K_V G^r_{\rm eff}/G^v_{\rm eff}$ from the product formulas [33]. When $G_+ \to \infty$, $K_+ \to K_V$.

Peselnick and Meister [8] had originally obtained all the results for hexagonal symmetry, except for one additional condition that permits c_{44} to be replaced in some circumstances by

$G^r_{\rm eff}$. This new condition was added later by Watt and Peselnick [10]. For trigonal symmetry, the general results $\mu_2 \leq \min(c_{44}, c_{66})$ and $\max(c_{44}, c_{66}) \leq \mu_1$, permitted simplification of these expressions. For tetragonal symmetry, the conditions depending on μ_3 [see (18)] were also added by Watt and Peselnick [10].

Implementation issues

Equation (63) has an obvious singularity if it ever occurs that $G_+ = G^v_{\rm eff}$. (The case $G_- = G^v_{\rm eff}$ can never occur except in the most trivial cases, where bounding methods are unnecessary.) Since this does happen in practice (known examples include: hexagonal cobalt, trigonal corundum, and both tetragonal urea and mercurous chloride), it is necessary to modify the numerical algorithm for these bounds slightly. To avoid this singularity, it is sufficient (and also consistent with spirit of the variational bounding methods) to make the replacement in these cases $G_+ = G^v_{\rm eff} + \delta$, where is δ is a small positive shift. This choice guarantees that the result is still an upper bound, but avoids the singularity. Any positive shift on the order of the experimental error in the crystalline elastic stiffness data should be sufficient to eliminate this purely numerical difficulty. But the choice made will also be reflected directly in the upper bounds on both bulk and shear modulus – so results being presented (for the upper bounds in these cases) may sometimes vary slightly from those of Watt and Peselnick [10].

However, the noted singularity does not affect the final results for self-consistent estimates at all — and so has nothing to do with any small discrepancies that might be found between present results and those of Gubernatis and Krumhansl [29]. It also means the preferred choices of the starting values for the self-consistent iteration scheme are generally the values for the lower PMW bounds on bulk and shear modulus, since these remain free of this issue.

Watt and Peselnick [10] actually did perform searches in the appropriate parameter ranges determined by (64)-(65) and (66)-(67). They found that the optimum choices were always quite close to the upper limits for G_-, and to the lower limits for G_+. We have not repeated these searches here, but choose instead to accept the limiting values as good estimates of the optimal values. Users who have exceptionally high quality crystal data to use as input, and who therefore want to obtain the very best estimates from these methods, should also implement a search routine.

The graphical structure of the algorithm for computing these bounds was illustrated originally by Watt and Peselnick [10].

Self-consistency relations for random polycrystalline aggregates can generally be obtained by making careful use of the Hashin-Shtrikman bounds themselves as constraints on these overall effective constants. The reader will find extended discussions of these ideas in the papers by Willis [30] and Berryman [33, 34]. Very minor modifications were needed for trigonal and tetragonal cases in the present work; resulting self-consistency conditions are closely related to formulas determining Hashin-Shtrikman bounds. The self-consistent values always necessarily (by construction) must lie inside these bounds.

Acknowledgments

Work performed under the auspices of the U.S. Department of Energy, at the Lawrence Berkeley National Laboratory under Contract No. DE-AC02-05CH11231. Support was provided specifically by the Geosciences Research Program of the DOE Office of Basic Energy Sciences, Division of Chemical Sciences, Geosciences and Biosciences, and is gratefully acknowledged by the author.

References

[1] W. Voigt, *Lehrbuch der Kristallphysik* (Teubner, Leipzig, 1928), p. 962.

[2] A. Reuss, "Berechung der Fliessgrenze von Mischkristallen," *Z. Angew. Math. Mech.* **9**, 49-58 (1929).

[3] R. Hill, The elastic behaviour of crystalline aggregate. *Proc. Phys. Soc.* **A65**, 349-354 (1952).

[4] G. Simmons and H. Wang, *Crystal Elastic Constants and Calculated Aggregate Properties: A Handbook* (The M. I. T. Press, Cambridge, Massachusetts, 1971).

[5] L. Thomsen, Elasticity of polycrystals and rocks. *J. Geophys. Res.* **77**, 315-327 (1972).

[6] J. D. Bass, Elasticity of Minerals, Glasses, and Melts, in *Mineral Physics and Crystallography* (American Geophysical Union, Washington, D. C., 1995), edited by T. J. Ahrens, pp. 45-63.

[7] Z. Hashin and S. Shtrikman, A variational approach to the theory of elastic behaviour of polycrystals. *J. Mech. Phys. Solids* **10**, 343-352 (1962).

[8] L. Peselnick and R. Meister, Variational method of determining effective moduli of polycrystals: (A) Hexagonal symmetry and (B) trigonal symmetry. *J. Appl. Phys.* **36**, 2879-2884 (1965).

[9] R. Meister and L. Peselnick, Variational method of determining effective moduli of polycrystals with tetragonal symmetry. *J. Appl. Phys.* **37**, 4121-4125 (1966).

[10] J. P. Watt and L. Peselnick, Clarification of the Hashin-Shtrikman bounds moduli of polycrystals with hexagonal, trigonal, and tetragonal symmetries. *J. Appl. Phys.* **51**, 1525-1531 (1980).

[11] J. P. Watt, Hashin-Shtrikman bounds on the effective elastic moduli of polycrystals

with orthorhombic symmetry. *J. Appl. Phys.* **50**, 6290-6295 (1979).

[12] J. P. Watt, Hashin-Shtrikman bounds on the effective elastic moduli of polycrytals wuth monoclinic symmetry, *J. Appl. Phys.* **51**, 1520-1524 (1980).

[13] J. P. Watt, Hashin-Shtrikman bounds on the effective elastic moduli of polycrystals with trigonal (3,$\bar{3}$) and tetragonal (4,$\bar{4}$,4m) symmetry. *J. Appl. Phys.* **60**, 3120-3124 (1986).

[14] J. P. Watt, Elastic properties of polycrystalline minerals: Comparison of theory and experiment. *Phys. Chem. Min.* **15**, 579-587 (1988).

[15] C. M. Salerno and J. P. Watt, Walpole bounds on the effective elastic moduli of isotropic multicomponent composites. *J. Appl. Phys.* **60**, 1618-1624 (1986).

[16] K. Schulgasser, Bounds on the conductivity of statistically isotropic polycrystals, *J. Phys. C: Solid State Phys.* **10**, 407-417 (1977).

[17] M. Avellaneda, A. V. Cherkaev, K. A. Lurie, and G. W. Milton, On the effective conductivity of polycrystals and a 3-dimensional phase-interchange inequality. *J. Appl. Phys.* **63**, 4989-5003 (1988).

[18] M. Avellaneda and G. W. Milton, Optimal bounds on the effective bulk modulus of polycrystals. *SIAM J. Appl. Math.* **49**, 824-837 (1989).

[19] G. W. Milton, *The Theory of Composites*, Cambridge University Press (Cambridge, UK, 2002).

[20] O. Weiner, Die Theorie des Mischkörpers für das Feld des stationären Strömung. Erste Abhandlung die Mittelswertsätze für Kraft, Polarisation und Energie. *Abhandlunger der mathematisch-physichen Klasse der Königlich Sächisiscehn Geselschaft der Wissenschaften* **32**, 509-604 (1912).

[21] E. Kröner, Bounds for effective elastic moduli of disordered materials. *J. Mech. Phys. Solids* **25**, 137-155 (1977).

[22] E. Kröner, Graded and perfect disorder in random media elasticity. *J. Engng. Mech. Div.* **106**, 889-914 (1980).

[23] J. G. Berryman, Measurement of spatial correlation functions using image processing techniques. *J. Appl. Phys.* **57**, 2374-2384 (1986).

[24] M. J. Beran, *Statistical Continuum Theories* (Interscience, New York, 1968), pp. 250–255.

[25] M. J. Beran, T. A. Mason, B. I. Adams, and T. Olson, Bounding elastic constants of an orthotropic polycrystal using measurements of microstructure. *J. Mech. Phys. Solids* **44**, 1543-1563 (1996).

[26] C. H. Arns, M. A. Knackstedt, W. V. Pinczewski, and E. J. Garboczi, Computation of linear elastic properties from microtomographic images: Methodology and agreement between theory and experiment. *Geophysics* **67**, 1396-1405 (2002).

[27] J. D. Eshelby, The determination of the elastic field of an ellipsoidal inclusion, and related problems. *Proc. Roy. Soc. London A* **241**, 376-396 (1957).

[28] R. Hill, A self-consistent mechanics of composite materials. *J. Mech. Phys. Solids* **13**, 213-222 (1965).

[29] J. E. Gubernatis and J. A. Krumhansl, Macroscopic engineering properties of polycrystalline materials: Elastic properties. *J. Appl. Phys.* **46**, 1875-1883 (1975).

[30] J. R. Willis, Variational and related methods for the overall properties of composites. in C.-S. Yih (ed.), *Advances in Applied Mechanics* (Academic Press, New York, 1981), pp. 1–78.

[31] T. Olson and M. Avellaneda, Effective dielectric and elastic constants of piezoelectric polycrystals. *J. Appl. Phys.* **71**, 4455-4464 (1992).

[32] T. R. Middya and A. N. Basu, Self-consistent T-matrix solution for the effective elastic

properties of noncubic polycrystals. *J. Appl. Phys.* **59**, 2368-2375 (1986).

[33] J. G. Berryman, Bounds and self-consistent estimates for elastic constants of random polycrystals with hexagonal, trigonal, and tetragonal symmetries. *J. Mech. Phys. Solids* **53**, 2141-2173 (2005).

[34] J. G. Berryman, Bounds and self-consistent estimates for elastic constants of polycrystals composed of orthorhombics or crystals with higher symmetries. *Phys. Rev. E* **83**, 046130 (2011).

[35] J. F. Nye, *Physical Properties of Crystals: Their Representation by Tensors and Matrices* (Oxford Science Publications, Oxford, UK, 1985).

[36] L. D. Landau and E. M. Lifshitz, *Theory of Elasticity* (Butterworth Heineman, Oxford, UK, 1986), p. 32.

[37] T. C. T. Ting, *Anisotropic Elasticity: Theory and Applications* (Oxford University Press, New York, 1996), pp. 53–56.

[38] T. Iitaka, K. Hirose, K. Kawamura, and M. Murakami, The elasticity of the $MgSiO_3$ post-perovskite phase in the earth's lowermost mantle. *Nature* **430**, 442-445 (2004).

[39] D. J. Weidner, H. Wang, and E. Ito, Elasticity of orthoenstatite. *Phys. Earth Planetary Inter.* **17**, P7-P13 (1978).

[40] D. J. Weidner and E. Ito, Elasticity of $MgSiO_3$ in the ilmenite phase. *Phys. Earth Planetary Inter.* **40**, 65-70 (1985).

[41] T. Tsuchiya and J. Tsuchiya, Structure and elasticity of Cmcm Ca IrO_3 and their pressure dependences:*Ab intitio* calculations. *Phys. Rev. B* **76**, 144119 (2007).

[42] R. E. G. Pacalo and D. J. Weidner, Elasticity of majorite, $MgSiO_3$ tetragonal garnet. *Phys. Earth and Planetary Inter.* **99**, 145-154 (1997).

[43] M. J. P. Musgrave, *Crystal Acoustics: Introduction to the Study of Elastic Waves and*

Vibrations in Crystals (Acoustical Society of America, AIP, New York, 2003), p. 281.

[44] R. M. Wentzcovich, B. B. Karki, S. Karto, and C. R. S. Da Silva, High pressure elastic ansiotropy of $MgSiO_3$ perovskite and Geophysical implications, *Earth Planetary Sci. Lett.* **164**, 371-378 (1998).

[45] R. M. Wentzcovitch, B. B. Karki, M. Cococcioni, and S. de Gironcoli, Thermoelastic properties of $MgSiO_3$-perovskite: Insights on the nature of the earth's lower mantle. *Phys. Rev. Lett.* **92**, 018501 (2004).

[46] T. Tsuchiya, J. Tsuchiya, K. Umemoto, and R. M. Wentzcovich, Phase transition in $MgSiO_3$ perovskite in the earth's lower mantle. *Earth Planetary Sci. Lett.* **224**, 241-248 (2004).

[47] K. Niwa, T. Yagi, and K. Ohgushi, Elasticity of $CaIrO_3$ with perovskite and post-perovskite structure. *Phys. Chem. Minerals* **38**, 21-31 (2011).

[48] F. D. Murnaghan, The compressibility of media under extreme pressures. *Proc. Nat. Acad. Sci. USA* **30**, 244-247 (1944).

[49] F. Birch, Finite elastic strain of cubic crystals. *Phys. Rev.* **71**, 809-824 (1947).

[50] E. Knittle and R. Jeanloz, Synthesis and equation of state of (Mg, Fe) SiO_3 perovskite to over 100 gigapascals. *Science* **235**, 668-670 (1987).

[51] M. Avellaneda and G. W. Milton, Optimal bounds on the effective bulk modulus of polycrystals. *SIAM J. Appl. Math.* **49**, 824-837 (1989).

[52] M. Avellaneda, A. V. Cherkaev, L. V. Gibiansky, G. W. Milton, and M. Rudelson, A complete characterization of the possible bulk and shear moduli of planar polycrystals. *J. Mech. Phys. Solids* **44**, 1179-1218 (1996).

Table 1. Elastic stiffness constants, Voigt-Reuss-Hill averages of bulk and shear modulus, and densities ρ for certain orthorhombic crystals of $MgSiO_3$, including the three varieties: protoenstatite, enstatite, and perovskite. Data from Bass [6], at room temperature and pressure. All elastic constants are in units of GPa.

	$MgSiO_3$		
	Protoenstatite	Enstatite	Perovskite
c_{11}	213.	224.7	515.
c_{22}	152.	177.9	525.
c_{33}	246.	213.6	435.
c_{12}	76.	72.4	117.
c_{13}	59.	54.1	117.
c_{23}	70.	52.7	139.
c_{44}	81.	77.6	179.
c_{55}	44.	75.9	202.
c_{66}	67.	81.6	175.
K_{vrh}	111.9	107.8	245.4
G_{vrh}	63.0	75.7	184.2
ρ (Mg/m^3)	3.052	3.198	4.108

Table 2. Elastic stiffness constant bounds and estimates for three examples quoted in Table 1, for the orthorhombic crystals of $MgSiO_3$, which comes in three varieties: protoenstatite, enstatite, and perovskite. Data from Bass [6], at room temperature and pressure, with constants in units of GPa.

	$MgSiO_3$		
	Protoenstatite	Enstatite	Perovskite
G_V	65.5	76.2	184.7
G_{HS}^+	63.1	75.7	184.0
G_{SC}	63.1	75.7	184.0
G_{HS}^-	63.1	75.5	184.0
G_{vrh}	63.0	75.7	184.0
G_{GM}	63.0	75.6	184.0
G_R	60.6	75.2	183.2
K_V	113.4	108.3	246.8
K_{HS}^+	112.1	107.8	246.1
K_{SC}	112.1	107.8	246.1
K_{HS}^-	112.1	107.7	246.1
K_{vrh}	111.9	107.8	246.1
K_{GM}	111.9	107.7	246.1
K_R	110.4	107.3	245.4

Table 3. Elastic stiffness constants and Voigt-Reuss-Hill averages of the bulk (K) and shear moduli (G) for the orthorhombic crystals of $MgSiO_3$, including two varieties: post-perovskite, perovskite, with each measured (or computed) at two different confining pressures. Data from Iitaka *et al.* [38]. All elastic constants are in units of GPa.

	$MgSiO_3$			
	Perovskite		Post-Perovskite	
c_{11}	852.	909.	1175.	1270.
c_{22}	1068.	1160.	862.	937.
c_{33}	1033.	1128.	1157.	1264.
c_{12}	461.	520.	366.	425.
c_{13}	368.	410.	289.	329.
c_{23}	391.	434.	437.	493.
c_{44}	340.	363.	264.	291.
c_{55}	265.	278.	242.	264.
c_{66}	312.	339.	368.	412.
K_{vrh}	596.0	654.2	594.8	660.0
G_{vrh}	295.9	314.1	306.3	332.1
ρ (Mg/m^3)	4.93	5.54	5.38	5.52
Pressure (GPa)	100.	120.	100.	120.

Table 4. Elastic stiffness constant bounds and estimates for the four Table 3 examples, of orthorhombic crystals of $MgSiO_3$ in two varieties: perovskite and post-perovskite. All elastic constants in units of GPa.

	$MgSiO_3$			
	Perovskite		Post-Perovskite	
G_V	298.9	318.2	314.9	341.7
G_{vrh}	295.9	314.1	306.3	332.1
G_{GM}	295.9	314.1	306.2	331.9
G^+_{HS}	296.1	314.4	306.0	331.8
G_{SC}	296.1	314.4	306.0	331.8
G^-_{HS}	296.1	314.4	306.0	331.8
G_R	292.9	310.0	297.7	322.4
K_V	599.2	658.3	597.6	662.8
K^+_{HS}	596.4	654.8	595.1	660.3
K_{SC}	596.4	654.8	595.1	660.3
K^-_{HS}	596.4	645.8	595.1	660.3
K_{vrh}	596.0	654.2	594.8	659.9
K_{GM}	596.0	654.2	594.8	659.9
K_R	592.9	650.1	592.0	657.0
Pressure (GPa)	100.	120.	100.	120.

Table 5. Elastic stiffness constants and Voigt-Reuss-Hill averages of the bulk (K) and shear moduli (G) for the crystals of $MgSiO_3$, for two varieties: trigonal ilmenite (with 7 independent constants, *i.e.,* $c_{66} = [c_{11} - c_{12}]/2)$), and tetragonal majorite (with 7 constants). Data for ilmenite from Weidner and Ito [40]. Data for majorite from Pacalo and Weidner [42]. All elastic constants are in units of GPa.

	$MgSiO_3$	
	Ilmenite	Majorite
c_{11}	472.0	286.4
c_{33}	382.0	280.1
c_{12}	168.0	83.0
c_{13}	70.0	104.9
c_{14}	27.0	
c_{16}		1.4
c_{25}	24.0	
c_{44}	106.0	85.0
c_{66}	152.0	93.2
K_{vrh}	212.0	159.8
G_{vrh}	132.0	89.7
ρ (Mg/m^3)	3.792	3.517

Table 6. Elastic stiffness constant bounds and estimates for two examples quoted in Table 5, for the trigonal (7 constants) and tetragonal (7 constants) crystals of $MgSiO_3$, which are called ilmenite and majorite, respectively. Ilmenite data are from Weidner and Ito [40]. Majorite data are from Pacalo and Weidner [42]).

	$MgSiO_3$	
	Ilmenite	Majorite
G_V	140.7	90.0
G_{HS}^{+}	135.2	89.8
G_{SC}	132.5	89.7
G_{vrh}	132.3	89.7
G_{GM}	132.0	89.7
G_{HS}^{-}	131.0	89.7
G_R	123.9	89.5
K_V	215.8	159.8
K_{HS}^{+}	213.0	159.8
K_{vrh}	212.3	159.8
K_{GM}	212.3	159.8
K_{SC}	211.8	159.8
K_{HS^-}	211.2	159.8
K_R	208.8	159.7

Table 7. Elastic stiffness constants, and Voigt-Reuss-Hill averages of bulk and shear modulus for certain orthorhombic crystals of $CaIrO_3$, including the two varieties: Cmcm (post-perovskite) phase and Pbnm (perovskite) phase. Data from Tsuchiya and Tsuchiya [41] at pressures P of 0 or 40 GPa. All elastic constants are in units of GPa.

	$CaIrO_3$			
	Cmcm		Pbnm	
c_{11}	388.	620.	248.	362.
c_{22}	241.	386.	359.	677.
c_{33}	386.	619.	319.	472.
c_{12}	121.	281.	204.	318.
c_{13}	85.	250.	115.	229.
c_{23}	149.	334.	162.	279.
c_{44}	67.	111.	79.	133.
c_{55}	46.	76.	42.	77.
c_{66}	64.	85.	97.	139.
K_{vrh}	189.	363.	202.	333.
G_{vrh}	73.	98.	68.	110.
P (GPa)	0.	40.	0.	40.

Table 8. Elastic stiffness constant bounds and estimates for the four examples of Table 7, of orthorhombic crystals of $CaIrO_3$ in two varieties: Cmcm and Pbnm and at two confining pressures: 0 and 40 GPa. All elastic constants are also in units of GPa.

	$CaIrO_3$			
	Cmcm		Pbnm	
K_V	191.67	372.78	209.78	351.44
K_{HS}^+	189.31	366.21	204.00	334.67
K_{SC}	189.30	366.18	203.97	334.63
K_{HS}^-	189.29	366.15	203.96	334.60
K_{vrh}	189.05	363.68	202.46	333.05
K_{GM}	189.03	363.57	202.32	332.54
K_R	186.43	354.59	195.14	314.65
G_V	79.40	105.07	73.27	115.47
G_{vrh}	73.50	97.92	68.48	109.78
G_{GM}	73.27	97.66	68.31	109.63
G_{HS}^+	72.54	97.36	68.86	109.87
G_{SC}	72.52	97.33	68.85	109.85
G_{HS}^-	72.50	97.31	68.84	109.84
G_R	67.61	90.78	63.69	104.09
Pressure (GPa)	0.	40.	0.	40.

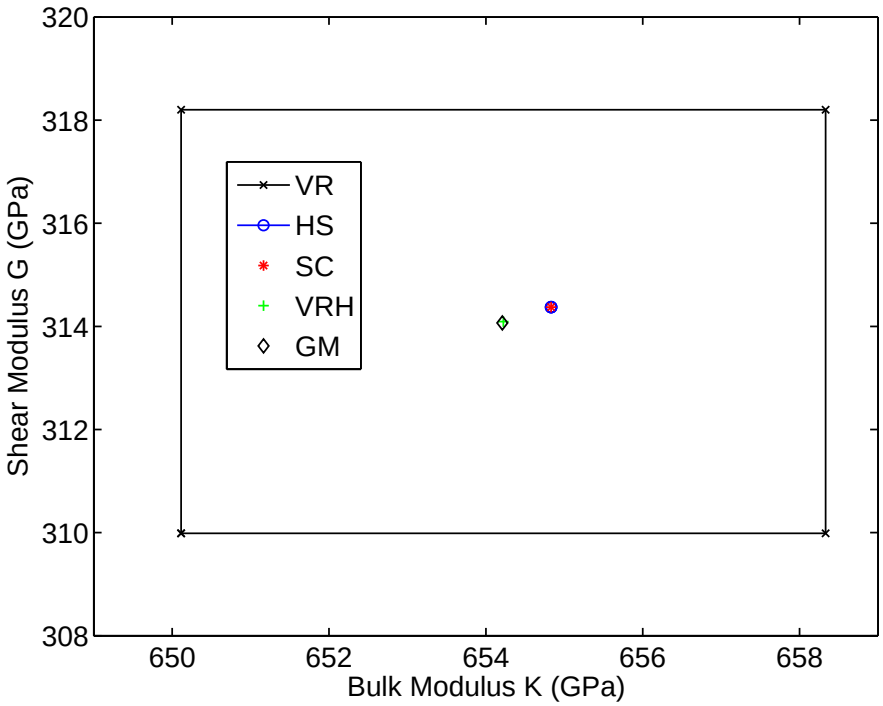

FIG. 1: Voigt-Reuss (VR) and Hashin-Shtrikman (HS) bounding boxes, with Self-Consistent (SC), Voigt-Reuss-Hill (VRH), and Geometric Mean (GM) estimates for effective elastic constants of polycrystalline (orthotropic) $MgSiO_3$ perovskite at confining pressure 120 GPa. Data from Iitaka *et al.* [38].

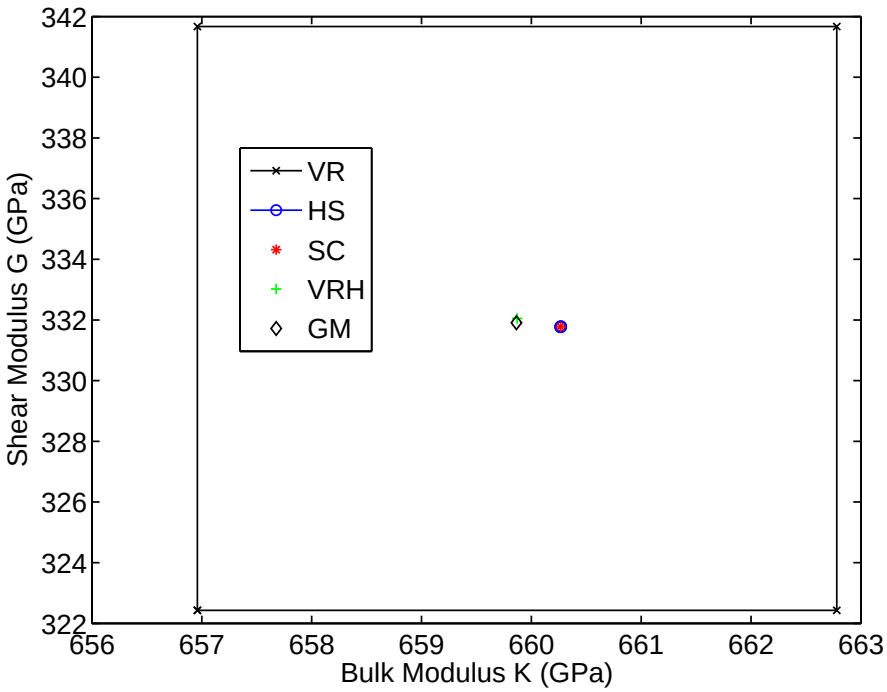

FIG. 2: Voigt-Reuss (VR) and Hashin-Shtrikman (HS) bounding boxes, with Self-Consistent (SC), Voigt-Reuss-Hill (VRH), and Geometric Mean (GM) estimates for effective elastic constants of polycrystalline (orthotropic) $MgSiO_3$ post-perovskite at confining pressure 120 GPa. Data from Iitaka *et al.* [38].

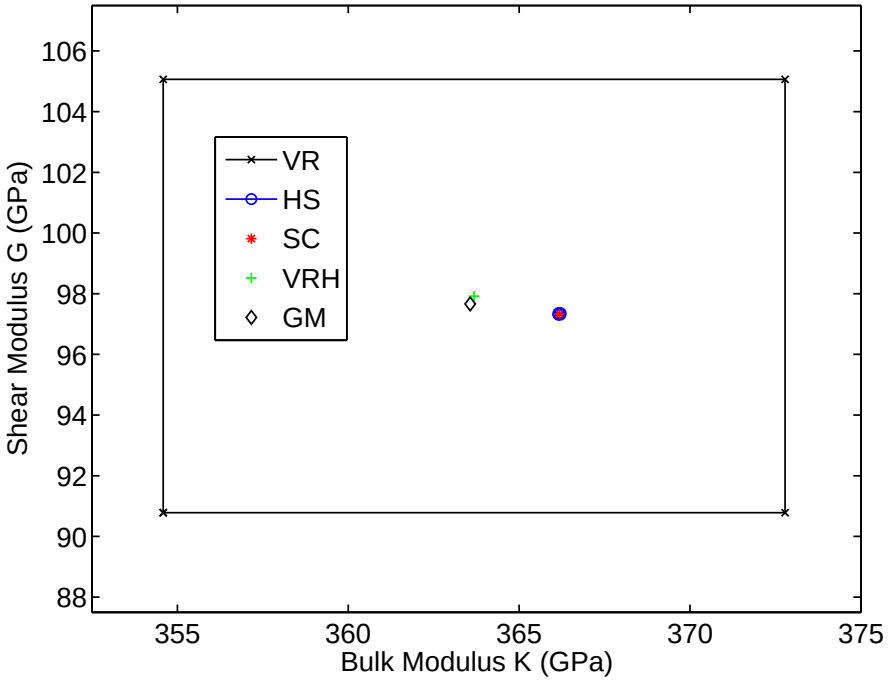

FIG. 3: Bulk and shear modulus bounds and estimates for $CaIrO_3$ post-perovskite (Cmcm) using data at $P = 40$ GPa of Tsuchiya and Tsuchiya [41].

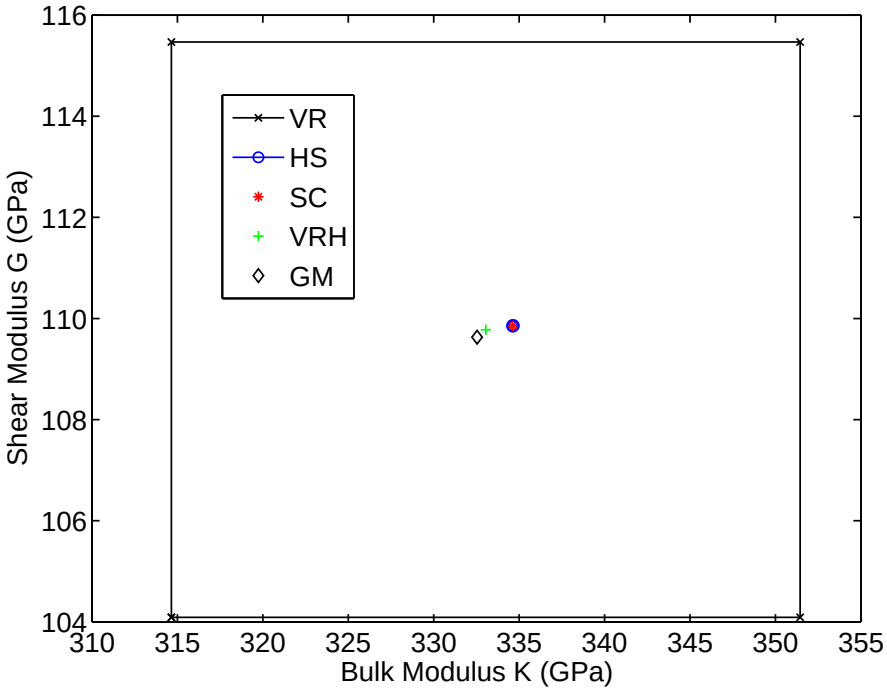

FIG. 4: Bulk and shear modulus bounds and estimates for $CaIrO_3$ perovskite (Pbnm) using data at $P = 40$ GPa of Tsuchiya and Tsuchiya [41].

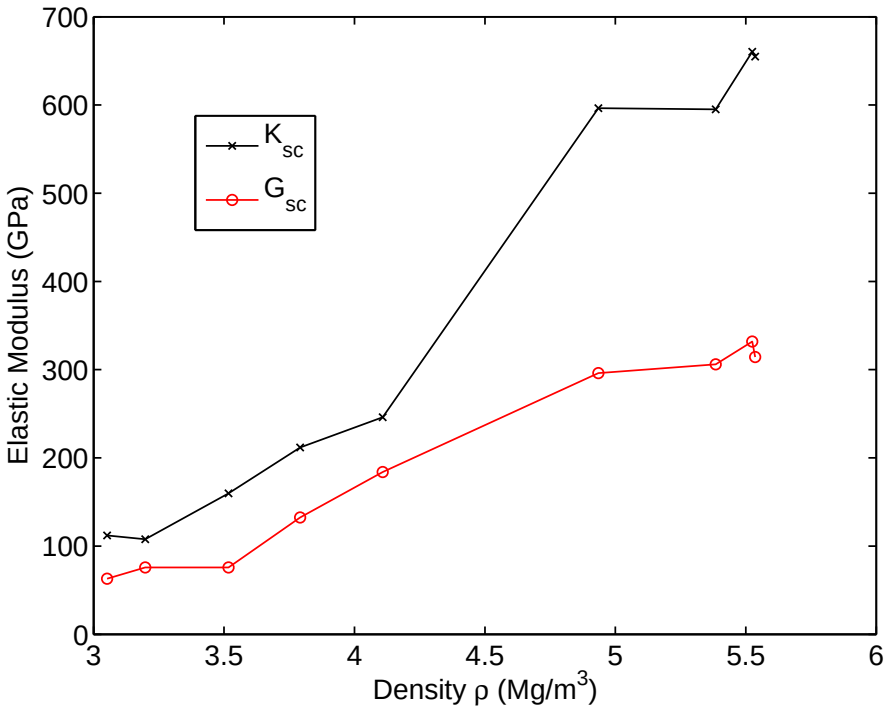

FIG. 5: Examples of the self-consistent values of bulk and shear modulus obtained for the predicted polycrystal behavior of $MgSiO_3$ composites having different structures, and also different densities. Plotting order from left to right is: orthorhombic protoenstatite (room T & P) and enstatite (room T & P), tetragonal majorite, trigonal ilmenite (100 GPa), and orthorhombic perovskite (room T & P), perovskite (100 GPa), post-perovskite (100 GPa), perovskite (120 GPa), and post-perovskite (120 GPa). While the values of these elastic moduli do in fact depend on both temperature and pressure, we use the single variable ρ (the density) as a proxy for the combination of the others in order to circumvent the need to use multidimensional plots. Information in Knittle and Jeanloz [50] was used to compute densities for the two higher pressure perovskite examples.